

## ELECTROCHEMICAL BEHAVIOUR OF Ti–6Al–4V ALLOY IN RINGER'S SOLUTION AFTER OXINITRIDING

O. V. TKACHUK<sup>1</sup>, I. M. POHRELYUK<sup>1</sup>, R. V. PROSKURNYAK<sup>1</sup>,  
J. GUSPIEL<sup>2</sup>, E. BELTOWSKA-LEHMAN<sup>2</sup>, J. MORGIEL<sup>2</sup>

<sup>1</sup> Karpenko Physico-Mechanical Institute of the National Academy of Sciences of Ukraine, Lviv, Ukraine;

<sup>2</sup> Institute of Metallurgy and Materials Science of the Polish Academy of Sciences, Krakow, Poland

Corrosion behaviour of nitrided and oxynitrided Ti–6Al–4V alloy in the Ringer's solution (simulated body fluid) at a temperature of 37°C was investigated. It was determined that corrosion resistance of the alloy in both cases was improved: the corrosion current density decreased, polarization resistance increased and corrosion potential became nobler.

**Keywords:** Ti–6Al–4V alloy, nitriding, oxynitriding, corrosion, Ringer's solution.

The Ti–6Al–4V titanium alloy is the most widely used for the orthopaedic and dental implants because of its high corrosion resistance and good mechanical properties [1–3]. Its corrosion resistance *in vitro* is caused by a strongly adherent oxide layer that is formed spontaneously on the alloy surface [4, 5]. However, when titanium alloy is implanted into physiological *in vivo* environment, the oxide stability may be affected, resulting in increased metal ion release and causing intoxication. Therefore there is an ongoing interest in modifying the implant surfaces [5, 6]. Thermodiffusion saturation with interstitial elements (nitrogen, oxygen) from a controlled gas medium is one of the methods of titanium alloys surface engineering [7]. Its important advantage is the possibility to provide high adhesion between the phase film and the metal matrix forming a gradient hardened diffusion layer.

The suitability of implants is evaluated in investigations of their corrosion resistance in physiological solutions which simulate the human body fluid [8]. The purpose of this work is to study the corrosion behaviour of nitrided and oxynitrided Ti–6Al–4V alloy in the Ringer's solution (simulated body fluid) at a temperature of 37°C.

**Materials and methods.** The cylindrical samples of Ti–6Al–4V alloy with a diameter of 8 mm and a height of 2 mm were investigated. The samples were mechanically ground by different grades of SiC emery papers, polished by diamond pastes to obtain a surface roughness of  $R_a = 0.2 \mu\text{m}$ . After polishing the samples were cleaned ultrasonically in alcohol and dried.

Nitriding of Ti–6Al–4V alloy was performed in the reaction chamber with a nitrogen gas medium at a nitrogen partial pressure of  $10^5$  Pa. The nitriding temperature was 850°C, and isothermal exposure in nitrogen was 5 h. Commercially pure nitrogen was used. The oxygen and moisture in the nitrogen atmosphere were removed by filtering the gas through a silica gel filter and heating the titanium chips at 50°C above the saturation process temperature. The oxygen content in the nitrogen was  $\leq 0.01\%$ , whereas the content in unpurified nitrogen was about 0.5%. The samples were heated to the nitriding temperature in a vacuum of  $10^{-3}$  Pa to remove the natural oxide films and avoid the formation of new ones during heating. After the isothermal exposure the samples were cooled in nitrogen to 500°C. Then the chamber was evacuated.

The oxynitriding of Ti–6Al–4V alloy was carried out by the putting the controlled oxygen-containing medium into the reaction chamber at the final stage of the nitriding: during cooling from 850 to 500°C. The oxygen partial pressure was 0.1 Pa.

The phase composition of the surface layers after nitriding and oxynitriding was investigated using a diffractometer DRON-3.0 with  $\text{CuK}\alpha$ -radiation at a voltage of 30 kV and a current of 20 mA. The tube focusing system was made using the Bragg–Brentano method. Titanium oxynitride was identified with application of the standard diffraction pattern obtained in accordance with the model by Levi et al. [9].

The corrosion resistance of the nitrided and oxynitrided Ti–6Al–4V alloy was evaluated at a temperature of  $37\pm 0.5^\circ\text{C}$  in an air-saturated Ringer's solution simulating the human body fluid. The electrochemical tests were carried out with application of an AUTOLAB PG Stat 302N potentiostat/galvanostat. The measurements were carried out with a standard three-electrode measuring system including platinum electrode as counter electrode, sample as a working electrode, and a saturated calomel electrode as a reference one. The surface area of the titanium samples exposed to the electrolyte was  $0.5\text{ cm}^2$ . Open circuit potential (OCP) had been measuring for two hours. The anodic and cathodic polarization curves were recorded using a sweep potential test in the range of  $\pm 150\text{ mV}$  with respect to the OCP, with a scanning rate of  $1\text{ mV/s}$ . The corrosion current density ( $i_{\text{corr}}$ ) and corrosion potential ( $E_{\text{corr}}$ ) were determined based on the Tafel relation using NOVA ver. 2.1.2 software.

**Results and discussion.** The nitride film of golden colour is formed on the surface of Ti–6Al–4V alloy as a result of thermodiffusion saturation with nitrogen. According to the results of the X-ray phase analysis (Fig. 1), it contains TiN and  $\text{Ti}_2\text{N}$  phases. TiN phase represented by (111), (200), (220), (311) and (222) reflections is predominant. In addition to the nitride phases, in the diffraction spectrum there are the lines of  $\alpha$ -Ti with the increased interplane distances, indicating the formation of the solid solution of nitrogen in titanium which separates the nitride film and the matrix alloy.

After modification of the titanium nitride by oxygen the alloy surface has a grey colour with a violet (lilac) tint which indicates indirectly the presence of the titanium oxynitrides [10]. According to the X-ray phase analysis, the oxynitride phase is represented by (111) reflection of  $\text{TiN}_x\text{O}_{1-x}$  of the weak relative intensity. Titanium dioxide in the rutile modification is also found on the alloy surface. This is confirmed by the (110), (101), (111), (211), (220) and (202) reflections of  $\text{TiO}_2$ . In addition the peaks of  $\text{Ti}_2\text{N}$  and  $\alpha$ -Ti phases are presented in the diffraction spectrum.

It is known that the OCP value varies with the immersion time in the corrosion environment due to changes on the surface material, and indicates its tendency to electrochemical oxidation [11]. Fig. 2 presents changes of the open circuit potentials (OCP) against time for the tested Ti–6Al–4V samples in the Ringer's solution at  $37^\circ\text{C}$ . All OCP are in the negative values.

For the untreated Ti–6Al–4V alloy the OCP decreases from  $-0.110$  to  $-0.150\text{ V}$  with further increase and stabilization at  $-0.078\text{ V}$  (Fig. 2, curve 1). A sharp decrease of the OCP can indicate the dissolution of the natural oxide film with its subsequent oxidation. The OCP stabilizes at  $-0.134\text{ V}$ .

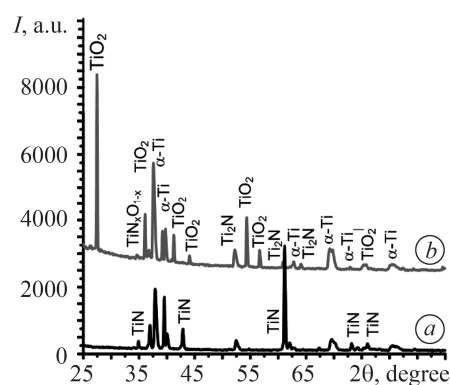


Fig. 1. Diffraction spectra taken from the surface of nitrided (a) and oxynitrided (b) Ti–6Al–4V alloy.

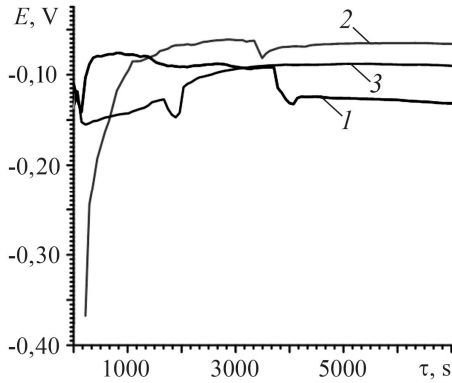


Fig. 2. Open-circuit potential vs time curves of untreated (1), nitrated (2) and oxynitrated (3) Ti-6Al-4V alloy in the Ringer's solution at 37°C.

For the nitrated alloy for the immersion in the solution to 1000 s, the OCP increases from  $-0.370$  to  $-0.056$  V (Fig. 2, curve 2). Obviously this is due to the oxidation of the nitride film. The OCP stabilizes at  $-0.066$  V. With formation of the nitride film on the surface, the potential is nobler by  $-0.068$  V compared to the untreated alloy (Table 1), which improves the corrosion properties.

For the oxynitrated alloy, as for the nitrated one, the OCP is nobler compared to the untreated alloy (Table 1). It should be noted also that for the oxynitrated alloy the OCP is situated in the region of lower potentials (Fig. 2, curve 3) compared to the nitride one. It

can indicate a lower corrosion resistance of the coating. Thus, nitriding and oxynitriding improve the anticorrosion properties of the alloy.

**Table 1. Corrosion parameters of the untreated, nitrated and oxynitrated Ti-6Al-4V alloy in the Ringer's solution at 37°C**

Ti-6Al-4V alloy	$E_{\text{corr}}$ , V	$i_{\text{corr}} \times 10^{-7}$ , A/cm <sup>2</sup>	$b_a$	$b_c$	$R_p$ , Ω cm <sup>2</sup>	$E_{\text{ocp}}$ , V
			V/dec			
untreated	-0.151	4.05	0.16	0.14	61500	-0.134
nitrated	-0.103	2.49	0.17	0.11	89500	-0.066
oxynitrated	-0.115	2.70	0.17	0.13	85500	-0.090

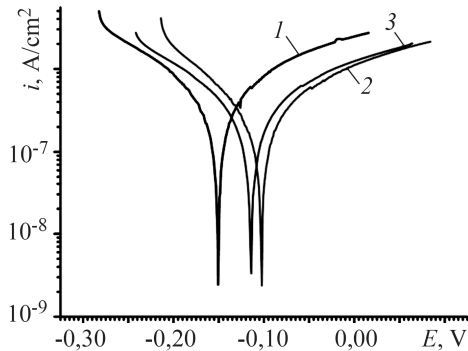


Fig. 3. Polarization curves of the untreated (1), nitrated (2) and oxynitrated (3) Ti-6Al-4V alloy in the Ringer's solution at 37°C after OCP measurements for 2 h.

Fig. 3 shows the polarization curves of Ti-6Al-4V alloy, taken in the Ringer's solution at a temperature of 37°C. The corrosion parameters derived from the Tafel plots, including the corrosion current density ( $i_{\text{corr}}$ ), corrosion potential ( $E_{\text{corr}}$ ), polarization resistance ( $R_p$ ), and the slope of anodic ( $b_a$ ) and cathodic ( $b_c$ ) polarization curves, are presented in Table 1. The untreated Ti-6Al-4V alloy is characterized by low corrosion resistance.

With the formation of the nitride coating on the surface (Fig. 3, curve 2), the corrosion current density decreases in

$\sim 1.6$  times, and the corrosion potential shifts by  $-0.048$  V to the values corresponding to the nobler ones compared to the untreated alloy (Table 1). The resistance of the nitride film increases in  $\sim 1.5$  times, thus improving the anticorrosion properties.

The corrosion behaviour of the oxynitrated alloy is deteriorated compared to the nitrated one (Fig. 3, curve 3). The corrosion current density increases and the corrosion potential shifts by  $-0.012$  V towards the more negative values. The film polarization resistance decreases (Table 1). It should be noted also that the oxynitrated alloy in

comparison with the untreated alloy tends to improve the corrosion resistance, as evidenced by the lower corrosion current density and corrosion potential by  $-0,037$  V to compare with the values corresponding to the nobler ones. The film polarization resistance increases (Table 1).

### CONCLUSIONS

It was determined that nitriding and oxynitriding improve the corrosion resistance of Ti–6Al–4V alloy in the Ringer's solution at a temperature of  $37^{\circ}\text{C}$  that simulates the tissue environment of the human body. The formed coatings provide a lower corrosion current density as well as a higher polarization resistance and a nobler corrosion potential compared to the untreated alloy.

*РЕЗЮМЕ.* Досліджено корозійну поведінку азотованого та оксинітрованого титанового сплаву Ti–6Al–4V у розчині Рінгера за температури  $37^{\circ}\text{C}$ , який моделює тканинну рідину людського організму. Встановлено, що в обох випадках підвищується корозійна тривкість сплаву: густина струму корозії знижується, поляризаційний опір зростає, а потенціал корозії ушляхетнюється.

*РЕЗЮМЕ.* Исследовано коррозионное поведение азотированного и оксинитрированного титанового сплава Ti–6Al–4V в растворе Рингера при температуре  $37^{\circ}\text{C}$ , который моделирует тканевую жидкость человеческого организма. Установлено, что в обеих случаях повышается коррозионная стойкость сплава: плотность тока коррозии снижается, поляризационное сопротивление увеличивается, а потенциал коррозии облагораживается.

1. *In situ* impedance spectroscopy study of the electrochemical corrosion of Ti and Ti–6Al–4V in simulated body fluid at  $25^{\circ}\text{C}$  and  $37^{\circ}\text{C}$  / V. A. Alves, R. Q. Reis, I. C. B. Santos, D. G. Souza, de F. T. Gonçalves, M. A. Pereira-da-Silva, A. Rossi, da L. A. Silva // *Corros. Sci.* – 2009. – **51**. – P. 2473–2482.
2. *Study of the biotribocorrosion behaviour of titanium biomedical alloys in simulated body fluids by electrochemical techniques* / M. K. Dimah, A. F. Devesa, V. Amigó Borrás, M. A. Igual // *Wear.* – 2012. – **294–295**. – P. 409–418.
3. *Engineering biocompatible implant surfaces. P. I: Materials and surfaces* / S. Bauer, P. Schmuki, von der K. Mark, and J. Park // *Prog. Mater. Sci.* – 2013. – **58**. – P. 261–326.
4. *Tailoring the surface properties of Ti–6Al–4V by controlled chemical oxidation* / F. Variola, J.-H. Yi, L. Richert, J. D. Wuest, F. Rosei, and A. Nanci // *Biomater.* – 2008. – **29**. – P. 1285–1298.
5. *Bacterial adhesion to titanium oxynitride (TiNOX) coatings with different resistivities: a novel approach for the development of biomaterials* / R. J. Koerner, L. A. Butterworth, I. V. Mayer, R. Dasbach, and H. J. Busscher // *Biomater.* – 2002. – **23**. – P. 2835–2840.
6. *Maury F. and Duminica F.-D. TiO<sub>x</sub>N<sub>y</sub> coatings grown by atmospheric pressure metal organic chemical vapor deposition* // *Surf. Coat. Technol.* – 2010. – **205**. – P. 1287–1293.
7. *Corrosion behaviour of thermodiffusion coatings on titanium implants in simulated body fluids* / O. Tkachuk, R. Proskurnyak, I. Pohrelyuk, and V. Fedirko // *Solid State Phenom.* – 2015. – **227**. – P. 503–506.
8. *Burstein G. T., Liu C., and Souto R. M. The effect of temperature on the nucleation of corrosion pits on titanium in Ringer's physiological solution* // *Biomater.* – 2005. – **26**. – P. 245–256.
9. *Levi G., Kaplan W. D., and Bamberger M. Structure refinement of titanium carbonitride (TiCN)* // *Mater. Lett.* – 1998. – **35**. – P. 344–350.
10. *Voitovich R. F. Oxidation of carbides and nitrides.* – К.: Наук. думка, 1981. – P. 192.
11. *Corrosion anisotropy of titanium deformed by the hydrostatic extrusion* / A. Chojnacka, J. Kawalko, H. Koscielny, J. Guspiel, A. Drewienkiewicz, M. Bieda, W. Pachla, M. Kulczyk, K. Sztwiertnia, E. Beltowska-Lehman // *Appl. Surf. Sci.* – 2017. – **426**. – P. 987–994.

Received 12.06.2018